Chinese Chemical Letters 32 (2021) 3531–3534

Contents lists available at ScienceDirect

Chinese Chemical Letters

journal homepage: www.elsevier.com/locate/cclet

Communication

Aggregation-induced emission and self-assembly of functional tetraphenylethene-based tetracationic dicyclophanes for selective detection of ATP in water

Chunyan Qin, Yawen Li, Qingfang Li, Chaochao Yan, Liping Cao*

College of Chemistry and Materials Science, Northwest University, Xi'an 710069, China

ARTICLE INFO

Article history:
Received 1 March 2021
Revised 6 May 2021
Accepted 8 May 2021
Available online 14 May 2021

Keywords:
Aggregation-induced emission
Dicyclophanes
Tetraphenylethene
Adenosine derivatives
Fluorescence

ABSTRACT

Functional dicyclophanes with various substituents (*e.g.*, NO_2, Br, OCH_3 and OH) were synthesized *via* one-pot S_N2 reaction. Dicyclophanes can form nanospheres *via* the head-to-tail self-assembly between the cavities and the TPE units to exhibit aggregation-induced emission (AIE) in aqueous solution. These AIE-active nanospheres with cationic feature exhibited selective recognition with fluorescence response for anionic ATP *via* electrostatic interactions and hydrophobic effects in water.

Adenosine derivatives are important biological compounds in all organisms [1]. For example, adenosine-5′-triphosphate (ATP), adenosine-5′-diphosphate (ADP), adenosine-5′-monophosphate (AMP) can transform with each other to realize energy storage and release [2], which ensures the energy supply for various life activities, such as energy transduction, metabolic process, extracellular signal transduction, DNA polymerization, cyclic adenosine monophosphate synthesis [3]. Therefore, the transformation between ATP and ADP/AMP plays a key role in providing energy for many processes of life. However, due to the strong hydration tendency of phosphate anion and the similar chemical structures, it is a difficult task to detect ATP from ADP or AMP in water [4]. Therefore, developing an efficient and convenient method to detect ATP is necessary and challenging. For example, Yang and co-workers reported the fluorescence response of a triarylboron compound to ATP, which was used to monitor the level of ATP *in vivo* and *in vitro* [5].

Supramolecular fluorescent macrocyclic systems can be assembled by mixing macrocyclic and guest components in solution *via* noncovalent interactions, such as van der Waals interactions, hydrophobic-hydrophilic interactions, hydrogen interactions, and electrostatic interactions. As a result, various cyclophanes have been widely exploited for the development of selective probes for a variety of guest molecules [6]. By introducing multiple functional groups, the fluorescent macrocyclic system can achieve large π-electron conjugation systems on the ring plane and endow the macrocyclic supramolecular aggregates or assembles with the diversity of photophysical properties [7]. Different functional groups can lead to great influence on the photophysical properties, such as emission wavelength, quantum yield, and fluorescence lifetime [8]. For examples, Chang and co-workers reported a series of naphthalimide derivatives with different optical properties such as quantum yield, emission color, and Stokes shift, due to the difference in substituents [9]. Tang and co-workers reported a series of pyridinium-functionalized tetraphenylethylene derivatives, and their emission could be turned from green to yellow to orange in the solid state [10]. On the other hand, the introduction of different functional groups into the molecular structure not only could adjust the luminescence of functional materials but also the self-assembled morphology, which further led to nano-functional materials with different electrical, optical, and magnetic properties [11,12]. Therefore, functionalization is an efficient method to improve the photophysical properties of fluorophores by using substituent effect.

Tetraphenylethene (TPE) and its derivatives are typical AIE-active luminescent groups [13]. Because of their high quantum yield in aggregation or solid state, convenient synthesis, and C_2 symmetry, they can be used as an ideal building block to construct cyclophanes, cages, and supramolecular organic frameworks (SOFs) with excellent fluorescence property [14–18]. Recently, we reported that a tetraphenylethene-based tetracationic dicyclophane (**1**), which can self-assemble into nanospheres with AIE prop-

* Corresponding author.
E-mail address: chcaoliping@nwu.edu.cn (L. Cao).

https://doi.org/10.1016/j.cclet.2021.05.006
1001-8417/

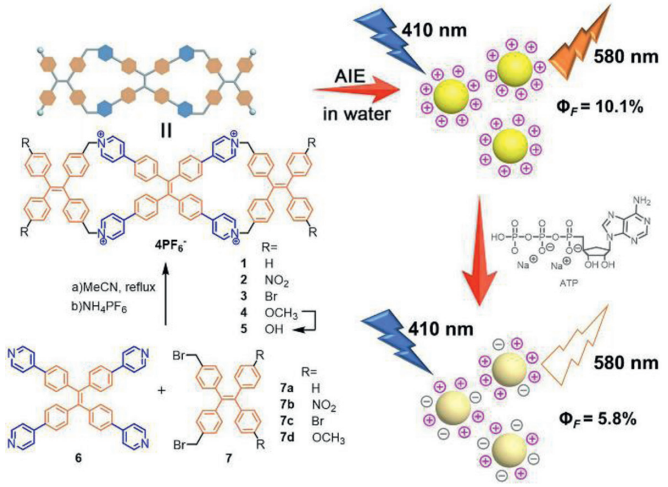

Scheme 1. Synthesis of tetraphenylethene-based tetracationic dicyclophanes **1**–**5** and schematic illustration of AIE and detection of ATP.

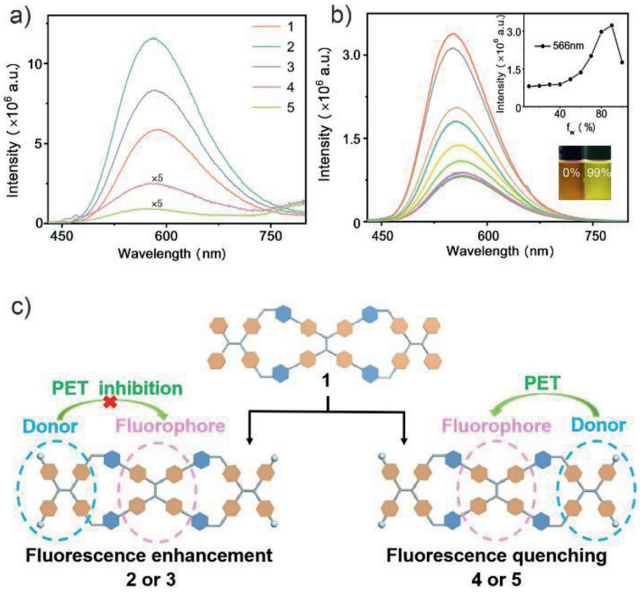

Fig. 1. (a) Fluorescence spectra of **1–5** in MeCN. (b) Fluorescence spectra of **2** (10 μmol/L) in various MeCN–H_2O mixture. Inset: Plot of maximum emission intensity of **2** *versus* water fraction. (c) Cartoon illustration of the mechanisms of fluorescence enhancement or quenching of **2–5**.

erty, combine with nile red to form light-harvesting nanospheres *via* hydrophobic effects in aqueous solution [16]. Herein, we design and synthesize a series of functional tetraphenylethene-based tetracationic dicyclophanes (**2**–**5**) with various substituents including electron-withdrawing (*e.g.*, NO_2 and Br) and electron-donating (*e.g.*, OCH_3 and OH) substituents to promote photophysical properties by controlling intramolecular photoinduced electron transfer (PET) [19]. These dicyclophanes can self-assemble into nanospheres *via* the head-to-tail self-assembly between the cavities and the TPE units to exhibit AIE property in water. In addition, nanospheres formed from dicyclophane **2** act as a single-molecule-based supramolecular platform can further exhibit fluorescence quenching when combined with ATP by electrostatic interactions to achieve selective detection of ATP in aqueous solution.

Different substituents such as NO_2, Br, OCH_3, and OH groups, which were selected to control the push-pull electronic effect in the structure of dicyclophanes. As shown in Scheme 1, tetrasubstituent dicyclophanes **2–4** with PF_6^- as counterions were synthesized from tetrapyridyl TPE **6** as central core and disubstituent bis(bromomethyl) TPEs **7b-7d** with NO_2, Br, or OCH_3 groups in the molar ratio of 1:2 *via* one-pot S_N2 reaction. And dicyclophane **5** with OH group was synthesized from compound **4** *via* a demethylation reaction. The compounds **2–5** were characterized by ^1H and ^{13}C NMR spectroscopy as well as electrospray ionization time-of-flight mass spectrometry (ESI-TOF-MS) (Figs. S1-S16 in Supporting information). UV–vis and fluorescence spectra of **1–5** displayed similar absorption bands and emission wavelengths, but different intensities and lifetimes (Figs. S17-S20 in Supporting information). Compared with unsubstituted **1, 2** and **3** with electron-withdrawing groups (*e.g.*, NO_2 and Br) displayed fluorescence enhancement with better absolute quantum yields (Φ_F) of 2.3% and 1.3% in MeCN, respectively (Fig. 1a, Fig. S19 and Table S1 in Supporting information). However, **4** and **5** with electron-donating groups (*e.g.*, OCH_3 and OH) exhibited fluorescent quenching with extremely low Φ_F value (< 0.1%) in MeCN, respectively (Fig. 1a, Fig. S19 and Table S1). These results indicated that fluorescent dicyclophanes **2** and **3** with electron-withdrawing groups could prohibit the intramolecular PET process between the outer TPE units as donor and the central TPE core as accepter, resulting in fluorescence enhancement, while the intramolecular PET from the donor to the fluorophore induce fluorescence quenching for **4** and **5** with electron donating groups (Fig. 1c).

Due to the AIE property of the TPE units, UV–vis and fluorescence spectra of **2** and **5** showed different absorption, emission intensities, and fluorescent colors in different solvent systems with various polarities and solubilities (Figs. S21-S24 in Supporting information). For example, when the $CHCl_3$ was gradually added to a solution of **2** in MeCN, the fluorescent intensity was gently increased (Fig. S21). And the fluorescent intensities of **3**–**5** were also increased when poor solvents (*e.g.*, $CHCl_3$, H_2O and CH_2Cl_2) were added (Figs. S22-S24). When compared with **1** (Φ_F = 13.8%), the fluorescence spectra of **2–5** in H_2O displayed red-shifted ($\Delta\lambda$ = 21-30 nm) with Φ_F value of 10.4%, 18.3%, < 0.1%, and < 0.1%, respectively (Fig. S19 and Table S4 in Supporting information), which were attributed to the aggregation in poor solvent. And the fluorescence lifetimes of **2–5** are longer than **1** in MeCN (Table S2 and Fig. S20). Furthermore, the fluorescent intensities of **2** also increased with the increase of water content in MeCN–H_2O mixture and the emission wavelengths have a slight blue shift due to solvent effects (Fig. 1b and Fig. S25 in Supporting information), while the fluorescent intensity of **5** remains almost constant (Fig. S27 in Supporting information). Besides, temperature-dependent fluorescence experiments implied that the fluorescence intensities of **2–5** decreased linearly as temperature gradually increased from 5 °C to 60 °C, indicating the aggregation of AIE-active **2–5** were achieved at lower temperature (Figs. S28-S31 in Supporting information). Finally, concentration-dependent fluorescence experiments (2.0 ~ 100 μmol/L) showed **2–4** in MeCN have low critical aggregation concentration of 25.8 μmol/L, 32.1 μmol/L and 26.7 μmol/L, respectively (Figs. S32-S34 in Supporting information). And **5** showed linear increase as the concentration increases (Fig. S35 in Supporting information). These results confirm that **2–5** have classic AIE property.

Fortunately, we obtained X-ray-quality crystals of **2** by slow vapor diffusion of diethyl ether into a solution of **2** in MeCN at room temperature (CCDC: 2061285). **2** has dual cavities formed mainly by 12 pyridinium/benzene rings in each cavity with the size of ~9.34 Å × ~12.6 Å, and all pyridinium and benzene rings are almost perpendicular to the plane of the cavities (Fig. 2a). And the double bonds of the outer TPE units are nearly vertical to the double bond of the central TPE. The two rotational conformations of TPEs including right-handed (*P*) and left-handed (*M*) rotational conformation are observed at two terminals in **2**. Meanwhile, the host-

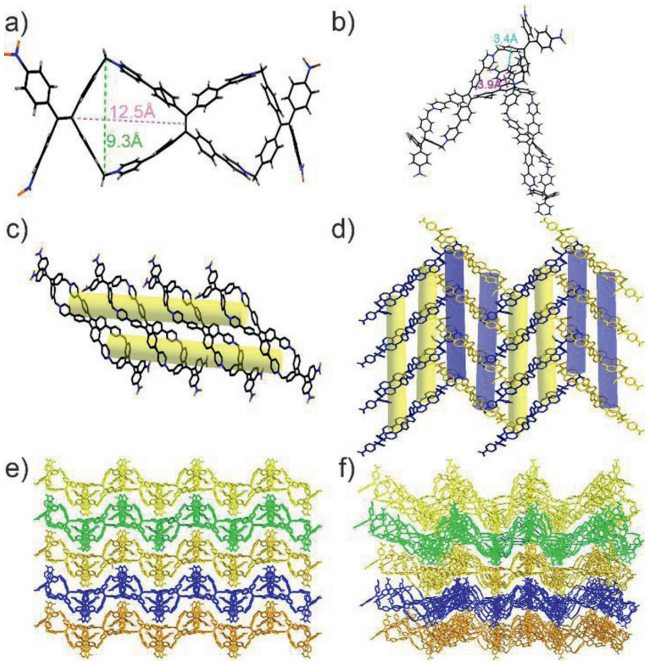

Fig. 2. X-ray crystal structure of **2**. (a) Single molecule, (b) side view from the b axis between two **2** molecules from neighboring nanotubes, (c) side view of the 1D dual nanotube from the b axis, (d) side view of 2D nanotubular layer from the b axis, and (e) top view of the 3D supramolecular framework from the c axis, (f) perspective view of the 3D framework from the c axis. Here, each 2D layers are colored by different colors for clarity.

guest interactions were observed between one terminal benzene ring with nitro group as the guest and one cavity of neighboring **2** as the host *via* CH···π (d = ~3.45 Å) and π···π (d = ~3.95 Å) interactions (Fig. 2b). More interestingly, a 3D supramolecular framework was stacked by **2** molecules. Firstly, the oblique **2** is arranged parallelly to form a 1D dual nanotube along the *a* axis (Fig. 2c). Secondly, neighboring 1D dual nanotubes with an opposite angle form a 2D nanotubular layer *via* head-to-tail interactions between the cavities and the TPE units in the zigzag alternate pattern along the *b* axis (Fig. 2d). Upon close inspection of this 2D nanotubular layer, two neighboring 1D dual nanotubes contact with each other through CH···π and π···π interactions. Finally, neighboring 2D nanotubular layers are stacked parallelly to form a 3D supramolecular framework (Figs. 2e and f).

Scanning electron microscopy (SEM) and transmission electron microscopy (TEM) were then used to investigate the formation of supramolecular nanospheres of **2**–**5** in MeCN or H_2O (1% MeCN). The SEM images of **2** showed the nanospheres with diameters of ~125 nm and ~63 nm in MeCN and H_2O (1% MeCN), while the irregular morphologies of **2** in other solvents were obtained (Fig. 3a and Fig. S36 in Supporting information), indicating the influence of the solvent effects on the self-assembled morphologies. Meanwhile, the TEM images further confirmed the morphology of the nanospheres with diameters of ~60 nm in H_2O (1% MeCN) (Fig. 3b). And the SEM and TEM images of **3**–**5** also showed nanosphere-like assemblies in MeCN or H_2O (1% MeCN) (Figs. S37-S43 in Supporting information). These results suggested that **2**–**5** can also self-assemble into nanospheres in MeCN or H_2O (1% MeCN). On the other hand, the average hydrodynamic diameters (D_H) of nanospheres formed from **2** (~94 nm), **3** (~79 nm), and **4** (~225 nm) in H_2O (1% MeCN) are significantly larger than the size of each signal molecule (Fig. S52 and Table S6 in Supporting information), which clearly indicates that dicyclophanes can form large supramolecular assemblies in H_2O (1% MeCN).

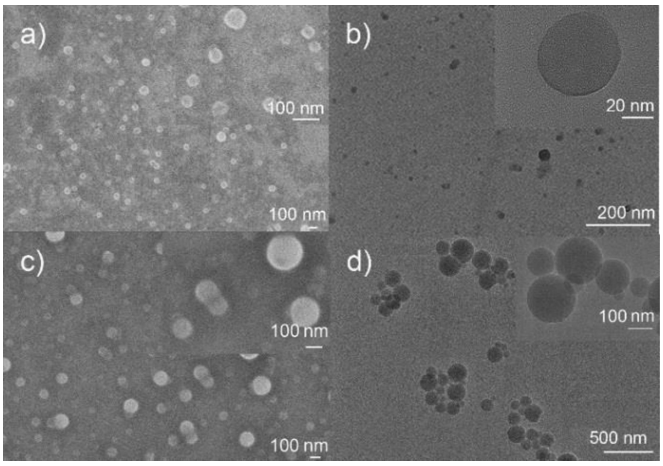

Fig. 3. SEM and TEM images of (a) and (b) **2** in H_2O (1% MeCN), (c) and (d) **2** + ATP (4.0 equiv.) in H_2O (1% MeCN). [**2**] = 10 μmol/L.

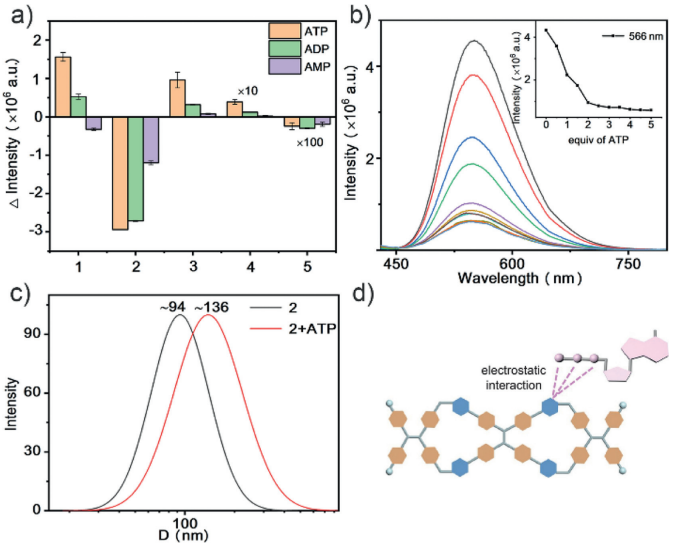

Fig. 4. (a) Fluorescence intensities (566 nm) of **1**–**5** with 4 equiv. of ATP, ADP or AMP. (b) Fluorescence spectra of **2** (10 μmol/L) in H_2O upon addition of ATP (0–5.0 equiv.). (c) DLS of **2** and **2** + ATP (4.0 equiv.) in H_2O (1% MeCN). [**2**] = 10 μmol/L. (d) Schematic illustration of the binding mechanism between dicyclophane and ATP.

The cationic pyridinium units of nanospheres can act as binding site to bind with anionic compounds with strong affinity *via* electrostatic interactions in aqueous solution. As expected, these nanospheres as a single-molecule-based supramolecular platform can exhibit selective responses with fluorescence enhancement or quenching to adenosine derivatives (*e.g.*, ATP, ADP and AMP), indicating that the supramolecular framework with cavities/interspaces in nanospheres can bind adenosine derivatives through electrostatic interactions and hydrophobic effects in aqueous solution. Usually, the fluorescence responses of nanospheres to ATP are more obvious than ADP and AMP, which may be attributed to the number of the phosphate groups of ATP, ADP and AMP (Fig. 4). Because ATP contains three negatively charged phosphate groups, its binding affinity with nanospheres is the strongest when compared with ADP and AMP, indicating that a more intimate binding affinity between nanospheres and the anionic molecules *via* electrostatic interactions in this case results in more fluorescence changes.

In UV–vis titration experiments of **1**–**5** with ATP in water, isosbestic points were observed, which suggested that ATP could be encapsulated in cavities/interspaces of nanospheres (Fig. 4a and Figs. S44-S47 in Supporting information). Interestingly, when ATP

was added to the solution of **2** in H_2O (1% MeCN), the fluorescence intensity was reduced greatly (Fig. 4b). It might contribute to the intermolecular PET process between positively-charged **2** and negatively-charged ATP occurred when ATP bound with **2** *via* electrostatic interactions. However, **1** and **3** display slightly fluorescence enhancements, these might contribute to the AIE effects induced by the complexation of **1** or **3** with ATP (Fig. 4a and Figs. S44-S47). It is a result of an equilibrium between the fluorescence enhancement mechanism of restriction intramolecular rotation (RIR) in the supramolecular aggregates and the fluorescence quenching mechanism of intermolecular PET based on the charge-transfer interaction between dicyclophanes and anionic guests. Owing to very weak fluorescence, **4** and **5** display very slight change (Fig. 4a and Figs. S44-S47). Moreover, the absolute quantum yields were 16.4%, 5.8%, 25.2%, $<$ 0.1% and $<$ 0.1% when ATP was added to the solution of **1–5** in H_2O (1% MeCN), respectively (Table S4 in Supporting information). These results suggest that **2** has selective detection with fluorescence response for ATP in water.

Meanwhile, the SEM and TEM images also demonstrated the cationic cavities/interspaces of supramolecular frameworks of **2**–**4** encapsulated ATP molecules to give larger nanospheres in solution (Figs. 3c and d and Figs. S48-S50 in Supporting information). To add ATP into a solution of **2** in H_2O (1% MeCN), the new nanospheres with an increase of average D_H of ~136 nm was obtained from nanosphere of **2** encapsulated ATP molecules (Fig. 4c). The fluorescence lifetimes of nanospheres and their complexes with ATP were similar (Fig. S51 and Table S5 in Supporting information). Similarly, the average D_H of **1, 3** and **4** also increased when ATP was added (Fig. S52 and Table S6 in Supporting information). When compared with **1**–**4**, the ζ potential of nanospheres from **1** to **4** with ATP have lower ζ potential, indicating that the positive nanospheres could be inserted by negative charges of ATP and the stability of AIE nanospheres bound with ATP decreases slightly (Table S6). Therefore, **2**–**4** as single-molecule-based supramolecular nanospheres could be encapsulated ATP molecules by electrostatic interactions to achieve selective detection of ATP in aqueous solution (Fig. 4d). The limits of detection (LOD) of **2**–**4** for the ATP were 0.16 μmol/L, 0.50 μmol/L and 0.87 μmol/L, respectively, indicating that **2** could sensitively recognize ATP (Figs. S53-S56 and Table S7 in Supporting information).

In summary, we have designed and synthesized four functional dicyclophanes **2–5** with different substituents (*e.g.*, NO_2, Br, OCH_3 and OH) to promote their fluorescence properties in aqueous solution. They have excellent AIE properties when self-assemble into nanospheres in aqueous solution. Dicyclophanes **2**–**3** with electron withdrawing groups prohibit the intramolecular PET process to induce fluorescence enhancement, while the intramolecular PET from the donor to the fluorophore result in fluorescence quenching for **4**–**5** with electron donating groups. Furthermore, dicyclophane molecules can self-assemble to nanospheres in aqueous solution. These nanospheres as a single-molecule-based supramolecular platform can exhibit fluorescence quenching/enhancing by combining with ATP *via* electrostatic interactions to achieve selective detection of ATP in aqueous solution. Therefore, this water-compatible supramolecular system with AIE property can be developed to a simple approach for the detection of biological molecules in biocompatible media.

Declaration of competing interest

The authors declare no conflict of interest.

Acknowledgments

This work was supported by the National Natural Science Foundation of China (Nos. 21971208 and 21771145), the Natural Science Basic Research Plan for Distinguished Young Scholars in Shaanxi Province of China (No. 2021JC-37), and the Fok Ying Tong Education Foundation (No. 171010).

Supplementary materials

Supplementary material associated with this article can be found, in the online version, at doi:10.1016/j.cclet.2021.05.006.

References

[1] Y. Zhou, Z. Xu, J. Yoon, Chem. Soc. Rev. 40 (2011) 2222–2235.
[2] (a) J.Y. Kwon, N.J. Singh, H. Kim, et al., J. Am. Chem. Soc. 126 (2004) 8892–8893;
(b) Z.C. Xu, J. Singh, L. Lim, et al., J. Am. Chem. Soc. 131 (2009) 15528–15533.
[3] A. Mishra, S. Dhiman, S.J. George, Angew. Chem. Int. Ed. (2021), doi:10.1002/anie.202006614.
[4] G. Yu, J. Zhou, J. Shen, G. Tang, F. Huang, Chem. Sci. 7 (2016) 4073–4078.
[5] X. Li, X. Guo, L. Cao, et al., Angew. Chem. Int. Ed. 53 (2014) 7809–7813.
[6] (a) D. Ramaiah, P.P. Neelakandan, A.K. Nair, R.R. Avirah, Chem. Soc. Rev. 39 (2010) 4158–4168;
(b) L. Wu, C. Huang, B.P. Emery, et al., Chem. Soc. Rev. 49 (2020) 5110–5139.
[7] (a) X. Ma, H. Tian, Chem. Soc. Rev. 39 (2010) 70–80;
(b) X. Ma, H. Tian, Acc. Chem. Res. 47 (2014) 1971–1981;
(c) X.L. Ni, S. Chen, Y. Yang, et al., J. Am. Chem. Soc. 138 (2016) 6177–6183.
[8] (a) P. Xu, Q. Qiu, X. Ye, et al., Chem. Commun. 55 (2019) 14938–14941;
(b) Y. Lei, W. Dai, J. Guan, et al., Angew. Chem. Int. Ed. 59 (2020) 16054–16060;
(c) X. Liu, Y. Qin, J. Zhu, et al., Chin. Chem. Lett. 32 (2021) 1537–1540;
(d) J.B. Pollock, G.L. Schneider, T.R. Cook, et al., J. Am. Chem. Soc. 135 (2013) 13676–13679.
[9] H.H. Lin, Y.C. Chan, J.W. Chen, et al., J. Mater. Chem. 21 (2011) 3170–3177.
[10] H.T. Feng, S. Zou, M. Chen, et al., J. Am. Chem. Soc. 142 (2020) 11442–11450.
[11] M.L. Saha, X. Yan, P.J. Stang, Acc. Chem. Res. 49 (2016) 2527–2539.
[12] (a) L. Cao, P. Wang, X. Miao, et al., J. Am. Chem. Soc. 140 (2018) 7005–7011;
(b) P. Wang, X. Miao, Y. Meng, et al., ACS Appl. Mater. Interfaces 12 (2020) 22630–22639.
[13] J. Li, J. Wang, H. Li, et al., Chem. Soc. Rev. 49 (2020) 1144–1172.
[14] H. Duan, Y. Li, Q. Li, et al., Angew. Chem. Int. Ed. 59 (2020) 10101–10110.
[15] (a) L. Cheng, K. Liu, Y. Duan, et al., CCS Chem 2 (2020) 2749–2751;
(b) L. Cheng, H. Zhang, Y. Dong, et al., Chem. Commun. 55 (2019) 2372–2375.
[16] (a) Y. Li, Y. Dong, L. Cheng, et al., J. Am. Chem. Soc. 141 (2019) 8412–8415;
(b) H. Nian, A. Li, Y. Li, et al., Chem. Commun. 56 (2020) 3195–3198;
(c) Q. Li, T. Cheng, S. Tan, et al., Chin. Chem. Lett. 31 (2020) 2884–2890.
[17] (a) Y. Li, Y. Dong, X. Miao, et al., Angew. Chem. Int. Ed. 57 (2018) 729–733;
(b) Y. Li, C. Qin, Q. Li, et al., Adv. Opt. Mater. 8 (2020) 1902154.
[18] Y. Li, Q. Li, X. Miao, et al., Angew. Chem. Int. Ed. 60 (2021) 6744–6751.
[19] J.L. Zhu, L. Xu, Y.Y. Ren, et al., Nat. Commun. 10 (2019) 4285.